

Spin-sensitive intersubband dynamics of optically generated carriers in semiconductor quantum wells

M. Vogel,¹ A. Vagov,¹ V. M. Axt,¹ A. Seilmeier,² and T. Kuhn³

¹*Theoretische Physik III, Universität Bayreuth, 95440 Bayreuth, Germany*

²*Experimentalphysik III, Universität Bayreuth, 95440 Bayreuth, Germany*

³*Institut für Festkörpertheorie, Universität Münster, 48149 Münster, Germany*

(Received 6 August 2009; revised manuscript received 17 September 2009; published 8 October 2009)

A theoretical analysis of the intersubband dynamics in undoped quantum wells is presented where spin-oriented carriers are initially generated by circularly polarized interband excitations. Subsequent resonant intersubband excitations induce Rabi rotations between the subbands resulting in a fast periodic modulation of the spin orientation in each subband. It is investigated whether pure spin modulations can be performed where the charge density of the subbands is kept constant when initially equal occupations of the two lowest conduction subbands with opposite spin orientations have been prepared. While this is the expected behavior for a three-band model of noninteracting particles it turns out that when the Coulomb interaction is taken into account the spin modulations are typically accompanied by corresponding modulations of the subband occupations. It is demonstrated that under realistic conditions it should nevertheless be feasible to realize a pure spin rotation in a given subband provided the intersubband excitations are sufficiently short or the carrier density is sufficiently low. Successive spin rotations are shown to decrease the degree of spin polarization even when spin-relaxation processes are neglected.

DOI: [10.1103/PhysRevB.80.155310](https://doi.org/10.1103/PhysRevB.80.155310)

PACS number(s): 78.47.Fg, 78.67.De, 42.65.-k

I. INTRODUCTION

Optically induced intersubband dynamics in semiconductor quantum wells attract much attention as it is a key ingredient for many ultrafast optoelectronic devices. Prominent examples are the quantum cascade laser¹⁻³ or quantum-well infrared or THz photodetectors.^{4,5} But also coherent aspects of the dynamics, many-body effects, and the identification of relevant relaxation mechanisms have been issues of interest.⁶⁻¹⁶ For intersubband experiments, where the carriers in the conduction bands are provided by doping, the available spin orientations are initially equally occupied. With these initial conditions optical spin orientation can be achieved in intersubband transitions that are driven by circularly polarized in-plane fields.¹⁷⁻¹⁹ However, such spin orientation effects result only from rather weak residual light-matter interactions which are typically about three orders of magnitude weaker than the strong couplings via the direct allowed intersubband dipole moments oriented along the growth direction.¹⁹ The latter can, however, not be used to induce a spin orientation. Intersubband dynamics are therefore usually insensitive to spin degrees of freedom in contrast to interband excitations, where circularly polarized pulses are routinely used to prepare charge densities with well-defined spin polarizations.²⁰ Recently, also the coherent ultrafast manipulation of spins in a modulation-doped quantum well by means of interband excitations has been demonstrated by performing coherently a complete electron-spin flip.²¹

In the present paper we analyze theoretically the laser-induced intersubband dynamics in undoped quantum wells where spin-oriented carriers have been created by circularly polarized interband excitations. With a suitable initial pulse sequence it can be achieved that the occupations of the two energetically lowest conduction subbands are initially equal

and have opposite spins. The aim of the paper is to explore the subsequent spin-dependent intersubband dynamics induced by laser pulses in resonance with the transition between these two conduction subbands. A main focus is the question whether the spin degrees of freedom in a given subband can be coherently manipulated independently from the charge degrees of freedom. It will turn out that many-body effects due to the Coulomb interaction have a decisive impact on the resulting dynamical properties. In particular, we find that under realistic conditions it is by no means trivial to drive the intersubband transitions in such a way that the spin expectation value in a given subband can be manipulated without affecting the corresponding total charge density. The identification of basic operations where spin and charge degrees of freedom can be controlled separately is, however, of central importance for the development of new applications where such basic operations may serve as building blocks, e.g., of spintronic devices.

II. MODEL

Our aim is to simulate the preparation of spin-polarized carriers by optical interband excitations (IB pulses) and the subsequent intersubband dynamics driven by laser pulses in resonance with the intersubband transitions (ISB pulses). We shall consider a generic semiconductor model which captures the main features of the physical situation that we want to describe. The parameters are chosen to be typical for GaAs-type materials. To be specific we model a quantum well of width $d=25$ nm with infinitely high barriers. We account for two spin degenerate conduction subbands (c_1, c_2) and one twofold-degenerate valence subband (v) of heavy-hole type (i.e., with total angular momentum components $m_J = \pm \frac{3}{2}$). All subbands are assumed to have parabolic dispersions. The effective in-plane masses in the conduction subbands

have been parameterized according to Ref. 22: $m_{xy} = m_{\text{bulk}}[1 + (2\alpha' + \beta')\epsilon]$, where m_{bulk} is the bulk conduction-band mass, α' and β' are nonparabolicity parameters, and ϵ is the confinement energy. Taking GaAs parameters with $\alpha' = 0.642$ 1/eV and $\beta' = 0.697$ 1/eV the resulting values for our structure are: $m_{c_1} = 0.068m_0$ and $m_{c_2} = 0.071m_0$, where m_0 is the bare electron mass. For the effective mass of the valence band we have taken an in-plane heavy-hole mass of $m_v = 0.11m_0$. Our main concern in this paper is the intersubband dynamics between the two lowest conduction subbands. For excitations near the band edges of these subbands the assumption of parabolic bands is quite realistic. The valence-band structure is usually more involved. Of course, the separation between the highest heavy-hole subbands and light-hole or splitoff subbands can be made large enough, e.g., by strain, such that these subbands are not excited by optical pulses in resonance with the transition between the uppermost valence- and the lowest-conduction subband. However, due to the large effective heavy-hole mass and the resulting small subband splitting in a real 25 nm quantum well more than one heavy-hole subband will contribute to optical transitions generated by IB pulses of 300 fs duration which are considered here. For simplicity and in order to reduce the numerical load we nevertheless model only a single valence subband, as for our scheme it is only important that it is possible to generate a certain density of spin-polarized carriers selectively in the lowest conduction subband. It does not matter from which valence subband the carriers originate. Furthermore, we have tested that the separation of the conduction subbands (25 meV for our parameters) is large enough to efficiently suppress excitations from the highest valence subband into the second conduction subband by spectral selection, even if such transitions were dipole allowed. For these reasons we expect that accounting for a larger number of valence subbands should only marginally affect the results presented in this paper. The quasi-two-dimensional Coulomb interaction between the carriers occupying the subband states of our model is accounted for on the mean-field level which describes many-body effects such as the depolarization shift and the Coulomb enhancement.^{16,23–25} Furthermore, we keep the dominant dipole couplings with the usual selection rules, i.e., a coupling to light circularly polarized in the x - y plane which drives the interband transitions between the valence and the lowest conduction band as well as a coupling to light polarized linearly in the growth direction which induces intersubband transitions between the two conduction subbands. For the IB transitions the rotating-wave approximation (RWA) is applied which is valid in this case because of the large separation of time scales between carrier wave and envelope. For the ISB transitions this condition is less well satisfied. Thus, the RWA is not used here.

To explore the dynamics of the system we adopt a momentum space density-matrix approach where equations of motion are solved for the following dynamical variables of interest,

$$C_c(\mathbf{k}) := \langle \hat{c}_{c,\mathbf{k}}^\dagger \hat{c}_{c,\mathbf{k}} \rangle \quad \text{electron subband occupation,}$$

$$D_v(\mathbf{k}) := \langle \hat{d}_{v,\mathbf{k}}^\dagger \hat{d}_{v,\mathbf{k}} \rangle \quad \text{hole subband occupation,}$$

$$Y_v^c(\mathbf{k}) := \langle \hat{d}_{v,-\mathbf{k}} \hat{c}_{c,\mathbf{k}} \rangle \quad \text{interband coherence,}$$

$$C_{c'}^c(\mathbf{k}) := \langle \hat{c}_{c',\mathbf{k}}^\dagger \hat{c}_{c,\mathbf{k}} \rangle \quad \text{intersubband coherence } c \neq c',$$

where $\hat{c}_{c,\mathbf{k}}^\dagger$ ($\hat{d}_{v,\mathbf{k}}^\dagger$) are Fermi operators that create an electron (hole) in subband c (v) with in-plane momentum $\hbar\mathbf{k}$; $\hat{c}_{c,\mathbf{k}}$ ($\hat{d}_{v,\mathbf{k}}$) are the corresponding destruction operators. On the mean-field level closed coupled equations of motion are obtained for the above dynamical variables by standard procedures [cf. Eqs. (24) and (75)–(77) of Ref. 26]. In addition to the Hamiltonian contributions to the dynamics of these variables relaxation processes are accounted for by suitable rates. Unless otherwise stated we use an interband dephasing time of $T_Y = 0.5$ ps and an intersubband decoherence time of $T_C = 3$ ps. As mentioned before, the well width of 25 nm corresponds in our model to a separation of the lowest two conduction bands of $\Delta E_C = 25$ meV. It is important for our study that ΔE_C is well below the energy of longitudinal-optical phonons E_{LO} (36.4 meV for GaAs) because for $\Delta E_C > E_{LO}$ occupations of the second conduction subband c_2 rapidly relax to the lowest subband c_1 by LO phonon emission. In this case, typical intersubband occupation relaxation times range from below 1 ps up to at most about 10 ps.^{27–30} Obviously, such short relaxation times are unfavorable for coherent manipulations of the subband occupations. In contrast, for $\Delta E_C < E_{LO}$ the intersubband scattering times are typically above 100 ps and may reach several hundred picoseconds at low temperatures.^{28,31–33} On the short-time scales that we shall discuss in the present paper, scattering times of a few hundred picoseconds can safely be ignored. Thus, in our case it is justified to neglect the interband relaxation of the occupation. We account, however, for spin-relaxation rates describing spin flips within the subbands. In particular, hole spin-relaxation times in wide quantum wells are typically of the order of only a few picoseconds^{34–36} while for narrow wells these times can be much longer.^{35,37} Here we use a value of $T_v^{\text{spin}} = 4$ ps as was measured in Ref. 34 for the hole spin-relaxation time. Electron-spin-relaxation times strongly depend on geometry, well width, and temperature. Typical values for GaAs-type quantum wells grown along the [001] direction are in the range between some tens to some hundreds of picoseconds^{38–40} while for samples grown along the [110] direction values in the nanosecond range have been reported.^{38,41–43} Here we shall use a value of $T_c^{\text{spin}} = 150$ ps which is well within the reported range but not too short for spin manipulations.

III. SPIN-SENSITIVE INTERSUBBAND DYNAMICS

Figure 1 sketches the scenario that will be analyzed in the present paper. The evolution through the states (a)–(d) is the preparation phase which aims at the preparation of equal carrier densities in the lowest two conduction subbands with opposite spin orientations. This is achieved by a sequence of three pulses. First, a circularly σ^+ -polarized IB pulse creates a density of spin-down electrons selectively in the lowest

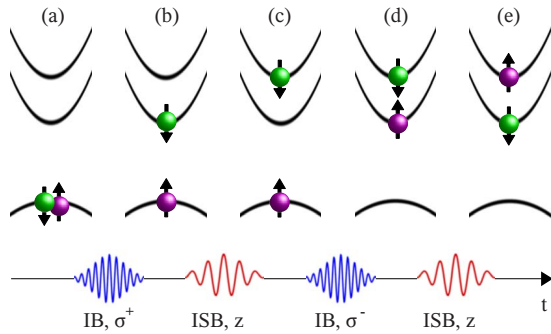


FIG. 1. (Color online) Preparation and manipulation scheme.

conduction subband (the quantization axis for the spin is the growth direction, which is taken to be the z direction). Then a linearly z -polarized ISB pulse is used to transfer these carriers to the second conduction subband by performing a π Rabi rotation. The third pulse is a circularly σ^- -polarized IB pulse which is adjusted in such a way to generate an equal amount of spin-up carriers in the lowest conduction subband resulting in the desired final state shown in Fig. 1(d). At first glance it might seem that a three pulse scheme is unnecessarily complicated and the desired preparation could be realized more easily by using two IB pulses with opposite circular polarizations, one tuned to the first and one to the second conduction subband. However, in such a setup the pulse tuned to the band edge of the second conduction band would inevitably also excite carriers in states with large k vectors in the lowest conduction band with the same spin orientation. Thus, equal carrier densities in the subbands with opposite spins could not be generated in this way.

When the preparation is finished additional ISB pulses may be used to further manipulate the carriers. As an example, in Fig. 1 this is indicated by a single additional pulse which performs a Rabi rotation in such a way that the spin orientation in each conduction subband is inverted. This operation would constitute an effective spin manipulation independent from charge manipulations as long as the charge density in each subband could be kept constant. We will come back to such spin-switching dynamics below.

Figure 2 shows results of simulations of the spin and charge dynamics where in the first part (up to about 5 ps) the system is prepared in a state with equal densities of carriers of opposite spin in the two lowest conduction subbands according to the scheme described above. Then a coherent spin manipulation is performed by applying an ISB pulse of 2 ps duration and a nominal pulse area of 6π . The top panel schematically indicates the envelopes of the pulses used. The panel in the middle displays the occupations of the lowest conduction subband calculated for a three-band model without Coulomb interaction while in the bottom panel corresponding results are shown where the Coulomb interaction has been taken into account. In both cases the IB pulses have been tuned in resonance to the band edge between the valence and the lowest conduction band while the ISB pulses were in resonance with the transition between the lowest two conduction subbands. The different curves represent occupations with spin up (\uparrow , dashes), spin down (\downarrow , dash dotted), and the total electron density ($\uparrow+\downarrow$, solid). It is clearly seen

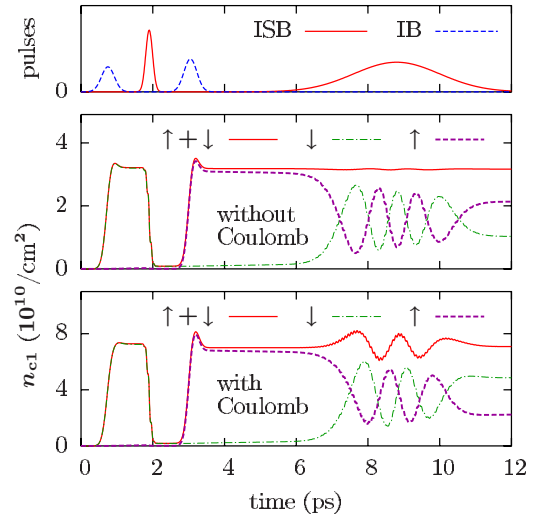


FIG. 2. (Color online) Top: pulse sequence. The durations of the pulses are [full width at half maximum (FWHM) of the intensity]: 300 fs for the IB pulses, 160 fs for the first ISB pulse, and 2 ps for the second ISB pulse. Middle and bottom occupations of the lowest conduction subband calculated with or without Coulomb interaction, respectively. The symbol $\uparrow(\downarrow)$ specifies the density with spin up (down) while $\uparrow+\downarrow$ marks the total subband density. Parameters: $T_Y=0.5$ ps, $T_C=3$ ps, $T_c^{\text{spin}}=150$ ps, and $T_v^{\text{spin}}=4$ ps.

that in both simulations with and without Coulomb interaction, after the preparation phase the lowest conduction subband contains practically only spin-up electrons, while all spin-down electrons that have been created by the first IB pulse have been transferred to the second subband, i.e., the desired preparation was successful, independently whether the calculations have been performed with or without Coulomb interaction. It should be noted that due to the fast hole spin relaxation, which takes place on the same time scale as the preparation process, the hole states with angular momentum component $m_j=-\frac{3}{2}$ are already noticeably occupied when the second IB pulse arrives although the first IB pulse generated with its σ^+ polarization only holes with $m_j=+\frac{3}{2}$. This reduces the absorption of the second IB pulse due to Pauli blocking effects. Thus, to obtain roughly equal densities of opposite spins in both subbands it is necessary to slightly increase the strength of the second IB pulse compared to the first one in order to compensate for these effects. Furthermore, we note that in the calculation where the Coulomb interaction has been neglected the total generated density is only roughly half as large as for the same IB pulse intensity in the full calculation. This is due to the well-known Coulomb enhancement in the absorption process. In order to make the preparation phase fast and efficient we have considered an ISB pulse of a total duration of 160 fs with a pulse area of π . For a pulse in resonance with the ISB transition, i.e., at 25 meV in our case, this corresponds roughly to a single cycle pulse with THz frequency. Due to substantial progress in laser technology it has recently become possible to generate intense single cycle pulses that are widely tunable in the THz regime.⁴⁴⁻⁴⁶ Thus, the realization of the preparation phase according to the protocol described above should be feasible.

Once spin-polarized carriers have been prepared in the conduction subbands one can try to manipulate the spin orientations in each subband with further ISB pulses. Let us first analyze Rabi rotations of the spin densities induced by an ISB pulse of 2 ps duration with pulse area 6π . The time evolution of the resulting densities in the lowest subband are shown in Fig. 2. For both calculations with and without Coulomb interaction it is found that the occupations of spin-up and spin-down electrons in the lowest subband indeed exhibit fast modulations reflecting the Rabi rotations induced by the ISB pulse. If a Rabi rotation starts with equal occupations of opposite spins in each subband it is tempting to assume that the number of carriers rotated from the lower to the upper band should equal the number of carriers that rotates down from the upper to the lower band. This is indeed the case in the calculation without Coulomb interaction, as seen in the middle panel of Fig. 2. Interestingly, however, the simulation where the Coulomb interaction has been included exhibits a qualitatively different behavior. Here, the modulation of the spin densities is accompanied by a modulation of the total subband occupation with the frequency of the Rabi oscillation.⁴⁷ This result can be understood by noting that the Coulomb interaction gives rise to k -dependent renormalizations of the ISB transition energies. An ISB pulse tuned to the onset of subband-to-subband transitions can thus not be in resonance with all transitions involved. Two further aspects are important: (a) the renormalizations induced by a given spin species (\uparrow or \downarrow) that arise from the Fock terms affect only the transition energies of that species; (b) the renormalizations depend on the subbands that are occupied because the occupations that enter the renormalizations are weighted with subband-dependent Coulomb matrix elements.^{26,48} As a result, the renormalization seen by a spin-up (spin-down) electron is different when the spin-up (spin-down) electron is in the upper or in the lower conduction subband. Thus the fraction of imperfect Rabi rotations due to detunings from the resonance condition depends on whether the carriers are rotated from the lower to the upper band or vice versa. This explains why the Coulomb interaction leads to a modulation of the total subband occupation during Rabi rotations between the lowest two conduction subbands even when the subbands are initially equally filled.

Besides giving rise to energy renormalizations the Coulomb interaction leads to a renormalization of the transition dipole moment. As can be seen from Fig. 2, in the case of ISB transitions this effectively modifies the pulse area. While in the case without Coulomb interaction the spin densities exhibit the behavior similar to the one expected for a 6π pulse, i.e., three more or less complete Rabi rotations, in the case with Coulomb interaction we observe only two and a half Rabi rotations corresponding to a 5π pulse.

Unlike the Coulomb-related modifications of the linear absorption spectra of undoped samples, the renormalizations of the ISB-transition energies scale with the carrier density. The carrier densities estimated for many typical existing ISB experiments are above 10^{11} $1/\text{cm}^2$.^{28,31} The excitation used for the calculations in Fig. 2 obviously yields carrier densities of that order. Thus, the curves shown so far correspond to typical and realistic conditions. However, according to the above interpretation it should be possible to suppress the

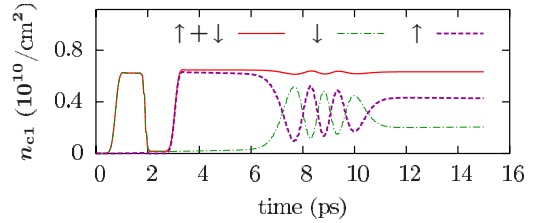


FIG. 3. (Color online) Occupations of the lowest conduction subband calculated as in Fig. 2 with Coulomb interaction but for lower intensities of the interband pulses.

oscillations of the total subband density by decreasing the excitation density. This is demonstrated in Fig. 3 where the strengths of the IB pulses have been reduced such that the resulting occupation of the lowest subband drops from $\sim 7 \times 10^{10}$ $1/\text{cm}^2$ as in Fig. 2 by more than a factor of 10 to $\sim 0.65 \times 10^{10}$ $1/\text{cm}^2$. All other parameters have been left unchanged. Now, also with Coulomb interaction the subband occupation exhibits only weak oscillations. Furthermore, we now also recover the three Rabi rotations expected for a 6π pulse. A systematic analysis of the density dependence (not shown) reveals that the density used for the simulation in Fig. 3 roughly marks the onset of a low-density regime: a further decrease in the density has practically no impact on the shape of the curves while with rising density the amplitude of the oscillations of the total subband occupation starts to grow continuously and the effective pulse area deviates increasingly from the nominal one.

Our interpretation of the origin of the oscillations of the total subband occupation has further implications. If the oscillations are due to Coulomb-induced detunings from the resonance condition then it should be possible to reduce the amplitude of the oscillations also by using shorter ISB pulses because due to the increasing spectral width of the shorter pulses transitions with an increasing amount of renormalization can be resonantly driven. To show that also this implication holds we have performed calculations where the carrier system generated by the same preparation protocol as above is now manipulated by a sequence of two 160 fs ISB pulses, each with a pulse area of π . All the other parameters are the same as in Fig. 2. Thus we now have a switching

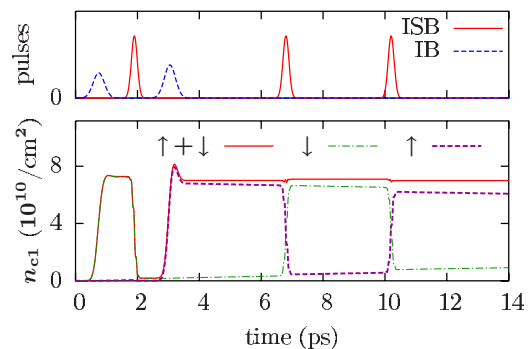


FIG. 4. (Color online) Occupations of the lowest conduction subband calculated as in Fig. 2 with Coulomb interaction except that the spin manipulation is performed with THz pulses of 160 fs duration (FWHM of the intensity).

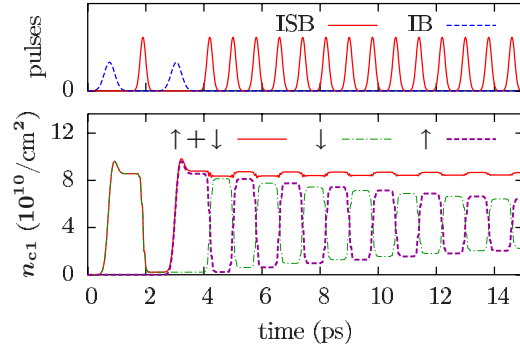


FIG. 5. (Color online) Occupations of the lowest conduction subband calculated with Coulomb interaction as in Fig. 4 except that the spin relaxations have been turned off and a larger number of spin switches is performed.

scenario similar to the one shown schematically in Fig. 1. The corresponding results are plotted in Fig. 4. Clearly, now it is possible to switch the spin orientation of the lowest subband on a sub-picosecond time scale practically without affecting its total occupation.

An other aspect seen both in Figs. 3 and 4 is the fact that the degree of spin polarization decreases with time. It is interesting to note that this decrease does not merely reflect the electron-spin-relaxation time of $T_c^{\text{spin}} = 150$ ps that was used in our simulation. In order to highlight this aspect we have performed calculations where the spin relaxation of electrons and holes have been completely switched off. Furthermore, instead of only two pulses a pulse train consisting of 160 fs ISB pulses has been used to manipulate the spin densities. The result is shown in Fig. 5. It is seen that with these short ISB pulses the spin orientation may be switched frequently with only minor impact on the total subband density. In between the ISB pulses there is now no longer any spin-relaxation mechanism in the model. Thus, the degree of spin polarization can change only during a switching process. Indeed, it decreases continuously with each additional switching step due to a combination of ISB decoherence present during the action of the pulses and residual detunings from the resonance condition. Both effects lead to imperfect Rabi rotations in the subspace of both spin species and, as a consequence, to an assimilation of the two spin densities.

IV. PUMP-PROBE SIGNALS

A standard method to monitor the dynamics of spin-dependent carrier densities is to perform pump-probe-type experiments with circularly polarized IB test pulses.⁴⁹ The idea is that the spin-dependent occupation leads to a blocking of the corresponding transition and is therefore reflected in the absorption of the test pulse. However, pump-probe signals measure nonlinear optical polarizations that are affected by various different influences. In addition to blocking-type contributions, which reflect the occupation dynamics, such signals may be influenced by coherent signal components arising from Coulomb-induced nonlinearities.^{50–52} For an experimental verification of the spin manipulation scheme proposed in the present paper it is thus of utmost importance to

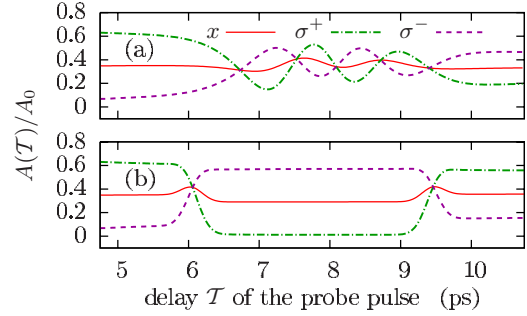


FIG. 6. (Color online) Absorption of a weak IB test pulse (300 fs FWHM of the intensity) as a function of the delay from the first interband pulse. (a) For excitations as in Fig. 2 (with Coulomb interaction) and (b) for excitations as in Fig. 4. The curves are normalized to the absorption of the unexcited sample.

know whether under the excitation condition considered here the predicted spin dynamics can be monitored in a pump-probe experiment. We have therefore performed simulations of experiments that measure the absorption of a weak test pulse arriving at the sample with a delay time τ with respect to the first IB pulse. We have considered a test pulse of 300 fs duration in resonance with the IB transition between the band edges of the highest valence and the lowest conduction subband. Such pulses are spectrally sufficiently narrow to exclude contributions from the second conduction subband which in a real quantum-well structure could occur due to transitions to lower-lying valence bands. The calculated absorption is plotted in Fig. 6 as a function of the delay time τ for three different polarizations of the test pulse: linearly x polarized (solid), circularly σ^+ polarized (dash dotted), and circularly σ^- polarized (dashed). Part (a) of the figure refers to the excitation conditions used for Fig. 2 (with Coulomb interaction) while part (b) corresponds to the conditions used for Fig. 4. It is clearly seen that the absorption of σ^\pm light closely follows the dynamics of the \uparrow and \downarrow occupations of the lowest conduction subband. The absorption of linear polarized light essentially reflects the behavior of the total subband occupation, except that the Rabi-type modulations are less pronounced in the absorption signal in Fig. 6(a) than in the corresponding density in Fig. 2. For the short ISB switching pulses this relation is reversed. Here, the absorption dynamics in Fig. 6(b) reacts more strongly to the switching pulses than the occupation in Fig. 4.

V. CONCLUSIONS

We have simulated the intersubband dynamics of spin-polarized carriers in an undoped semiconductor quantum well. It has been demonstrated that with a suitable sequence of two interband excitations with opposite circular polarizations and one linearly polarized intersubband excitation it should be possible to prepare a situation where the lowest conduction subbands are equally populated with carriers of opposite spin orientations. Further intersubband pulses can then be used to drive spin-sensitive intersubband dynamics. We have shown that with long ISB pulses a periodic modulation of the spin density in a given subband can be achieved.

However, due to Coulomb-induced renormalizations of the dynamics these modulations are typically accompanied by oscillations of the total subband density. It turned out that for low carrier densities or short ISB pulses it becomes nevertheless feasible to switch the spin orientations essentially without changing the total occupations of the subbands. In addition to the occupation dynamics we have simulated pump-probe-type experiments. The predicted spin rotations are shown to be experimentally accessible in such pump-probe measurements with circularly polarized probe pulses

tuned in resonance with the lowest interband transition. Our simulations of such experiments show that the fast spin modulations remain clearly visible under realistic conditions. By using linearly polarized test pulses one can monitor also the total subband occupation and thus decide experimentally whether spin and charge degrees of freedom have been controlled independently. According to our simulations it should be possible to realize a system where long-lived spin polarizations could be manipulated on short-time scales without significantly affecting the corresponding charge density.

-
- ¹C. Gmachl, F. Capasso, D. L. Sivco, and A. Y. Cho, *Rep. Prog. Phys.* **64**, 1533 (2001).
- ²J. Faist, F. Capasso, D. L. Sivco, C. Sirtori, A. Hutchinson, and A. Y. Cho, *Science* **264**, 553 (1994).
- ³R. Köhler, R. C. Iotti, A. Tredicucci, and F. Rossi, *Appl. Phys. Lett.* **79**, 3920 (2001).
- ⁴F. Castellano, R. C. Iotti, and F. Rossi, *Appl. Phys. Lett.* **92**, 091108 (2008).
- ⁵S. R. Schmidt, A. Seilmeier, and H. C. Liu, *J. Appl. Phys.* **91**, 5545 (2002).
- ⁶L. E. Vorobjev, V. Y. Panevin, N. K. Fedosov, D. A. Firsov, V. A. Shalygin, A. Seilmeier, S. R. Schmidt, E. A. Zibik, E. Towe, and V. V. Kapaev, *Semicond. Sci. Technol.* **21**, 1267 (2006).
- ⁷I. Waldmueller, W. W. Chow, and A. Knorr, *Phys. Rev. B* **73**, 035433 (2006).
- ⁸S. Butscher, J. Förstner, I. Waldmüller, and A. Knorr, *Phys. Rev. B* **72**, 045314 (2005).
- ⁹T. Shih, K. Reimann, M. Woerner, T. Elsaesser, I. Waldmüller, A. Knorr, R. Hey, and K. H. Ploog, *Phys. Rev. B* **72**, 195338 (2005).
- ¹⁰J. Li and C. Z. Ning, *Phys. Rev. Lett.* **93**, 087402 (2004).
- ¹¹J. Li and C. Z. Ning, *Phys. Rev. B* **70**, 125309 (2004).
- ¹²I. Waldmüller, J. Förstner, S.-C. Lee, A. Knorr, M. Woerner, K. Reimann, R. A. Kaindl, T. Elsaesser, R. Hey, and K. H. Ploog, *Phys. Rev. B* **69**, 205307 (2004).
- ¹³M. Woerner, R. A. Kaindl, F. Eickemeyer, K. Reimann, T. Elsaesser, A. M. Weiner, R. Hey, and K. H. Ploog, *Physica B* **314**, 244 (2002).
- ¹⁴R. A. Kaindl, M. Wurm, K. Reimann, M. Woerner, T. Elsaesser, C. Miesner, K. Brunner, and G. Abstreiter, *Phys. Rev. Lett.* **86**, 1122 (2001).
- ¹⁵R. A. Kaindl, S. Lutgen, M. Woerner, T. Elsaesser, B. Nottelmann, V. M. Axt, T. Kuhn, A. Hase, and H. Künzel, *Phys. Rev. Lett.* **80**, 3575 (1998).
- ¹⁶B. Nottelmann, V. M. Axt, and T. Kuhn, *Physica B* **272**, 234 (1999).
- ¹⁷S. D. Ganichev, S. N. Danilov, V. V. Bel'kov, E. L. Ivchenko, M. Bichler, W. Wegscheider, D. Weiss, and W. Prettl, *Phys. Rev. Lett.* **88**, 057401 (2002).
- ¹⁸S. A. Tarasenko, E. L. Ivchenko, V. V. Bel'kov, S. D. Ganichev, D. Schowalter, P. Schneider, M. Sollinger, W. Prettl, V. M. Ustinov, A. E. Zhukov, and L. E. Vorobjev, *J. Supercond.* **16**, 419 (2003).
- ¹⁹J. B. Khurgin, *Appl. Phys. Lett.* **88**, 123511 (2006).
- ²⁰*Optical Orientation*, edited by F. Meier and B. P. Zakharchenya (Elsevier, Amsterdam, 1984).
- ²¹C. Phelps, T. Sweeney, R. T. Cox, and H. Wang, *Phys. Rev. Lett.* **102**, 237402 (2009).
- ²²U. Ekenberg, *Phys. Rev. B* **40**, 7714 (1989).
- ²³Marie S-C. Luo, S. L. Chuang, S. Schmitt-Rink, and A. Pinczuk, *Phys. Rev. B* **48**, 11086 (1993).
- ²⁴D. E. Nikonov, A. Imamoğlu, L. V. Butov, and H. Schmidt, *Phys. Rev. Lett.* **79**, 4633 (1997).
- ²⁵J. Li and C. Z. Ning, *Phys. Rev. Lett.* **91**, 097401 (2003).
- ²⁶F. Rossi and T. Kuhn, *Rev. Mod. Phys.* **74**, 895 (2002).
- ²⁷A. Seilmeier, H.-J. Hübner, G. Abstreiter, G. Weimann, and W. Schlapp, *Phys. Rev. Lett.* **59**, 1345 (1987).
- ²⁸A. Seilmeier, M. Wörner, G. Abstreiter, G. Weimann, and W. Schlapp, *Superlattices Microstruct.* **5**, 569 (1989).
- ²⁹M. C. Tatham, J. F. Ryan, and C. T. Foxon, *Phys. Rev. Lett.* **63**, 1637 (1989).
- ³⁰J. Faist, F. Capasso, C. Sirtori, D. L. Sivco, A. Hutchinson, S. N. G. Chu, and A. Y. Cho, *Appl. Phys. Lett.* **63**, 1354 (1993).
- ³¹D. Y. Oberli, D. R. Wake, M. V. Klein, J. Klem, T. Henderson, and H. Morkoç, *Phys. Rev. Lett.* **59**, 696 (1987).
- ³²T. Müller, R. Bratschitsch, G. Strasser, and K. Unterrainer, *Appl. Phys. Lett.* **79**, 2755 (2001).
- ³³B. N. Murdin, W. Heiss, C. J. G. M. Langerak, S.-C. Lee, I. Galbraith, G. Strasser, E. Gornik, M. Helm, and C. R. Pidgeon, *Phys. Rev. B* **55**, 5171 (1997).
- ³⁴T. C. Damen, L. Viña, J. E. Cunningham, J. Shah, and L. J. Sham, *Phys. Rev. Lett.* **67**, 3432 (1991).
- ³⁵P. Schneider, J. Kainz, S. D. Ganichev, S. N. Danilov, U. Rössler, W. Wegscheider, D. Weiss, W. Prettl, V. V. Bel'kov, M. M. Glazov, L. E. Golub, and D. Schuh, *J. Appl. Phys.* **96**, 420 (2004).
- ³⁶J. Kainz, P. Schneider, S. D. Ganichev, U. Rössler, W. Wegscheider, D. Weiss, W. Prettl, V. V. Bel'kov, L. E. Golub, and D. Schuh, *Physica E (Amsterdam)* **22**, 418 (2004).
- ³⁷R. Ferreira and G. Bastard, *Phys. Rev. B* **43**, 9687 (1991).
- ³⁸Y. Ohno, R. Terauchi, T. Adachi, F. Matsukura, and H. Ohno, *Phys. Rev. Lett.* **83**, 4196 (1999).
- ³⁹R. S. Britton, T. Grevatt, A. Malinowski, R. T. Harley, P. Perozzo, A. R. Cameron, and A. Miller, *Appl. Phys. Lett.* **73**, 2140 (1998).
- ⁴⁰A. Tackeuchi, Y. Nishikawa, and O. Wada, *Appl. Phys. Lett.* **68**, 797 (1996).
- ⁴¹O. Z. Karimov, G. H. John, R. T. Harley, W. H. Lau, M. E. Flatté, M. Henini, and R. Airey, *Phys. Rev. Lett.* **91**, 246601 (2003).

- ⁴²S. Döhrmann, D. Hägele, J. Rudolph, M. Bichler, D. Schuh, and M. Oestreich, *Phys. Rev. Lett.* **93**, 147405 (2004).
- ⁴³V. V. Bel'kov, P. Olbrich, S. A. Tarasenko, D. Schuh, W. Wegscheider, T. Korn, C. Schüller, D. Weiss, W. Prettl, and S. D. Ganichev, *Phys. Rev. Lett.* **100**, 176806 (2008).
- ⁴⁴T. Bartel, P. Gaal, K. Reimann, M. Woerner, and T. Elsaesser, *Opt. Lett.* **30**, 2805 (2005).
- ⁴⁵A. Sell, A. Leitenstorfer, and R. Huber, *Opt. Lett.* **33**, 2767 (2008).
- ⁴⁶J. Hebling, K.-L. Yeh, M. C. Hoffmann, B. Bartal, and K. A. Nelson, *J. Opt. Soc. Am. B* **25**, B6 (2008).
- ⁴⁷The fast small-amplitude oscillations that are superimposed on the Rabi oscillations of the total subband occupation reflect counter-rotating signal components that are absent when the RWA is applied also to the ISB transitions.
- ⁴⁸T. Kuhn, in *Theory of Transport Properties of Semiconductor Nanostructures*, Electronic Materials Vol. 4, edited by E. Schöll (Chapman & Hall, London, 1998), Chap. 6, pp. 173–214.
- ⁴⁹M. J. Stevens, A. L. Smirl, R. D. R. Bhat, A. Najmaie, J. E. Sipe, and H. M. van Driel, *Phys. Rev. Lett.* **90**, 136603 (2003).
- ⁵⁰V. M. Axt and T. Kuhn, *Rep. Prog. Phys.* **67**, 433 (2004).
- ⁵¹G. Bartels, G. C. Cho, T. Dekorsy, H. Kurz, A. Stahl, and K. Köhler, *Phys. Rev. B* **55**, 16404 (1997).
- ⁵²V. M. Axt, K. Victor, and A. Stahl, *Phys. Rev. B* **53**, 7244 (1996).